



**PROCEEDINGS OF
THE FIRST INTERNATIONAL CONFERENCE
ON
SCIENCE AND ENGINEERING**

Volume - 1

**Electronics
Electrical Power
Information Technology
Engineering Physics**

**Sedona Hotel, Yangon, Myanmar
December 4-5, 2009**

**PROCEEDINGS OF THE
FIRST INTERNATIONAL CONFERENCE
ON
SCIENCE AND ENGINEERING**

Volume - 1

**Electronics
Electrical Power
Information Technology
Engineering Physics**

**Organized by
Ministry of Science and Technology**

**DECEMBER 4-5, 2009
SEDONA HOTEL, YANGON, MYANMAR**

ELECTRONIC ENGINEERING

Wideband Array for Monopulse Tracking Systems

Zaw Moe Aung^{#1}

[#]Department of Naval Architecture, Defence Services Technological Academy (D.S.T.A)
Pyin Oo Lwin, Union of Myanmar

¹zawmoeaung@gmail.com

Abstract— In this paper, a wideband monopulse antenna array with double-sided tapered slot antenna elements is designed. This antenna system can achieve two-dimensional monopulse performance, and printed structure is simple and cost effective. The new type of hybrid for wideband application is also proposed and designed. This paper includes measurement and computation of system characteristics, as well as simulation results of the array's field patterns and antenna system gain. The maximum null depth is -46 dB and the maximum gain is 14 dB at 14 GHz.

Keywords— Monopulse, hybrid, tapered slot antenna (TSA), comparator, wide band array, sum pattern, difference pattern.

I. INTRODUCTION

Satellite tracking and other tracking methods for radio-astronomy, radio direction-finding, wireless communication systems, wireless computer networks and other modern communication systems have often included monopulse capability for searching and tracking purposes.

In these fields of tracking systems, the need for antennas of increased angular accuracy has changed from sequential lobing and conical scan to simultaneous lobing or monopulse. The most common tracking techniques are lobe switching, conical scan and monopulse [1]. Among these techniques monopulse tracking is the most accurate electronic direction-finding technique [2]. Monopulse has been developed as a solution to overcome the erroneous angle indication and slow searching speed of the lobe switching and conical scan techniques used in tracking systems.

Monopulse is a technique in which information concerning the angular location of a source or target is obtained by comparison of signals received simultaneously in two or more antenna patterns.

microwave devices known as hybrids or hybrid junctions of which there are several different types. Fig.1 shows the basic structure of the monopulse antenna system.

The angular errors of the desired pointing angle are denoted as ΔH for the azimuth error, ΔE for the elevation error and the total received signal is usually denoted as the sum signal, Σ . The sum signal (Σ) of the antenna system in the figure is used on transmit and for range measurement on receive. The difference patterns (ΔH and ΔE) are produced on receive using a microwave hybrid circuit called a monopulse comparator.

Many different types of antennas can be used in monopulse system. The three main categories of antennas used are: lenses, reflectors and arrays, each of which can be subdivided into various types. In traditional monopulse systems, Cassegrain parabolic antennas or lens antennas are commonly applied. The monopulse comparator in such systems is usually very complicated and heavy.

Lightweight and low cost microstrip structures have been developed for the monopulse application. Naveed Ahsan designed an X-band microstrip monopulse antenna for monopulse tracking radar [3] and Wang developed a single-layer monopulse microstrip patch antenna array working in Ku-band [4]. In this paper, a wideband monopulse antenna array with double-sided tapered slot antenna elements is presented. Design procedure of Monopulse antenna system consists of two parts: design of radiating parts and design of monopulse comparator.

II. DESIGN OF TSA FOR MONOPULSE ARRAY

In this section TSA consisting of two metallization layers was proposed and the design procedure was presented. In 1974 Lewis [5] has proposed the TSA as a new member of the class of frequency independent antennas. The schematic of the tapered slot antenna TSA antenna is shown in Fig. 2.

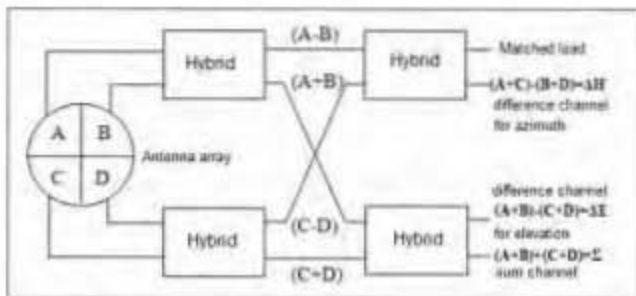


Fig. 1 Block diagram of monopulse antenna system

A typical monopulse antenna system consists of four antenna elements, from which a sum and two difference field patterns can be obtained. This requires use of certain passive

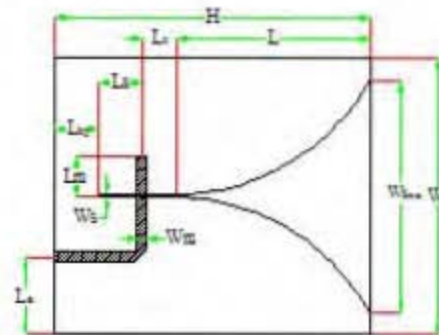


Fig. 2 Tapered slot antenna

In the TSA due to exciting microstrip line, field patterns are not symmetrical in both E and H-plane. To circumvent these problems, TSA consisting of two metallization layers was proposed and design data have been calculated. This new antenna is shown in Fig. 3.

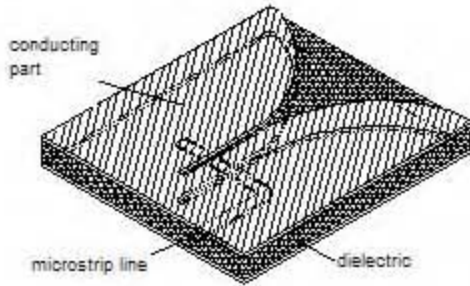


Fig. 3 Double-sided tapered slot antenna

Double-sided tapered slot antenna (TSA) is an end-fire travelling wave antenna. Like microstrip antennas, this TSA features low profile, light weight, easy fabrication by photoetching, conformal installation and compatibility with microwave integrated circuits (MIC). The antenna is formed by gradually flaring the strip conductors of the balanced microstrip on both sides of the dielectric substrate with respect to the antenna axis, thus allowing the antenna to be directly fed by a microstrip feed (Fig. 3).

In general, the design of TSA involves two major tasks: (1) the design of a broadband transition and feed structure with very wide frequency range and low return loss, and (2) determining the dimensions and shape of the antenna in accordance with the required beam width, side lobe, and back lobe etc. over the operating frequency range.

In TSA the energy in the traveling wave is tightly bound to the conductors when the separation is very small compared to the free space wavelength and becomes progressively weaker and was coupled to the radiation field as the separation is increased. To radiate electromagnetic energy at lowest frequency the aperture width of slot (see Fig. 2) must be

$$W_{s_{max}} \geq \lambda_{s_{max}} / 2 \quad (1)$$

where $\lambda_{s_{max}}$ - wavelength in dielectric with ϵ_r at lowest frequency f_{min} :

$$\lambda_{s_{max}} = \lambda_{0_{max}} / \sqrt{\epsilon_r} \quad (2)$$

where $\lambda_{0_{max}}$ - wavelength in free space at frequency f_{min} .

For the formation of only one maximum lobe array distance must be less than minimum operating wavelength. For the system without scanning:

$$W \leq \lambda_{0_{min}} \quad (3)$$

where $\lambda_{0_{min}}$ - wavelength in free space at maximum frequency f_{max} .

As $W \geq W_{s_{max}}$ from equations (1), (2), and (3) it can be clearly seen that width of antenna aperture should be

$$\lambda_{0_{min}} \geq W \geq \lambda_{0_{max}} / (2 \cdot \sqrt{\epsilon_r}) \quad (4)$$

Feeding a TSA requires transition between the slotline and other transmission media such as coplanar waveguide (CPW), microstrip line, and coaxial lines. Microstrip line is in widely use in power combining circuit. Since microstrip line is an unbalanced line and slotline is a balanced line, feeding a TSA with a microstrip line requires a balanced-to-unbalanced transition (balun) to avoid compromising the broadband antenna performance.

The transition and the corresponding transmission line model are shown in Fig. 2. The balun consists of four quarter-wave sections with the end open-circuited section extended past the centre of the slotline by about one quarter of a guided wavelength.

The proper selection of the stripline/slotline transition is crucial to the wide-band performance of the array. For good matching in wideband, length of microstrip L_m should be one quarter of a guided wavelength $\lambda_m/4$ and length of slot line transition L_s should be approximately $\lambda_s/4$.

$$\text{There } \lambda_m = \frac{\lambda_0}{\sqrt{\epsilon_{rem}}} ; \lambda_s = \frac{\lambda_0}{\sqrt{\epsilon_{res}}}$$

λ_m - effective wavelength in microstrip line;

λ_s - effective wavelength in slot line;

ϵ_r - effective dielectric constant of substrate.

For microstrip line:

$$\epsilon_{rem} = 0.5 \cdot [\epsilon_r + 1 + (\epsilon_r - 1) \cdot F] \quad (5)$$

where

$$F = [1 + 12 \cdot t / W_m]^{-0.5} + 0.04 \cdot [1 - W_m / t]^2 \text{ when } W_m / t \leq 1.$$

$$F = [1 + 12 \cdot t / W_m]^{-0.5} \text{ when } W_m / t \geq 1.$$

$$\text{For slot line: } \epsilon_{res} = 0.5 \cdot [\epsilon_r + 1] \quad (6)$$

where

$$\lambda_s = \lambda_0 / \sqrt{\epsilon_{res}} = \lambda_0 / [2 / (\epsilon_r + 1)]^{0.5} \rightarrow (\lambda_0 / \lambda_s)^2 \equiv \epsilon_{res}$$

Designed parameters of double sided (three-layered) tapered slot antenna, obtained in the process of parametric optimization [6], are shown in Table 1.

TABLE I
OPTIMIZED DESIGN PARAMETERS OF DOUBLE-SIDED TSA

Parameters	ϵ_r	L	L_{bp}	L_m	L_s	L_t	H
(mm)	4	15	3.75	3	3.75	0	22.5
Parameters	R	W_m	W_s	$W_{s_{max}}$	W	h_s	t_m
(mm)	17	1.2	0.56	18.6	20	3	0.1

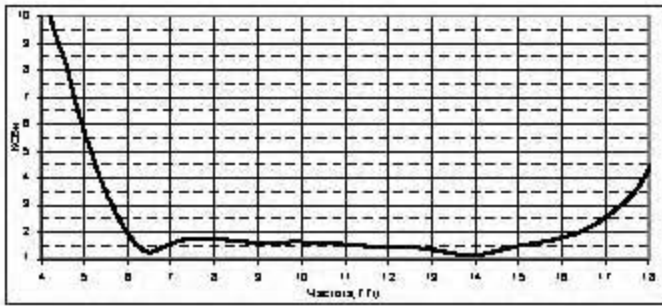


Fig. 4 VS WR vs. frequency curve

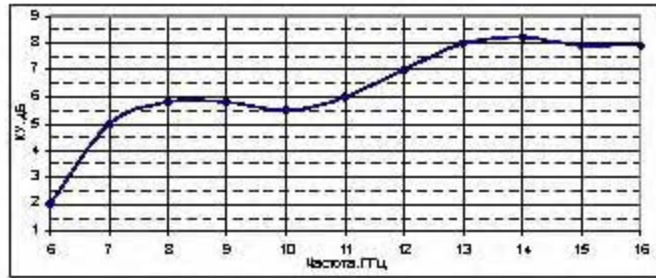


Fig. 5 Gain vs. frequency curve

Fig. 4 shows the voltage standing wave ratio of antenna within the frequency range of 4GHz to 18GHz. The gain of antenna vs. frequency is plotted in Fig. 5. Field patterns at various frequencies in E- and H-plane are shown in Fig. 6 and 7 respectively.

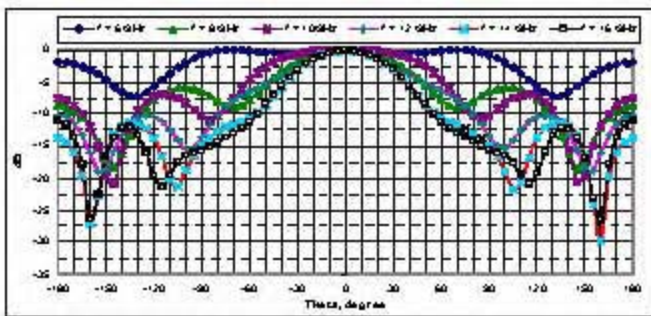


Fig. 6 Field pattern of antenna in E-plane

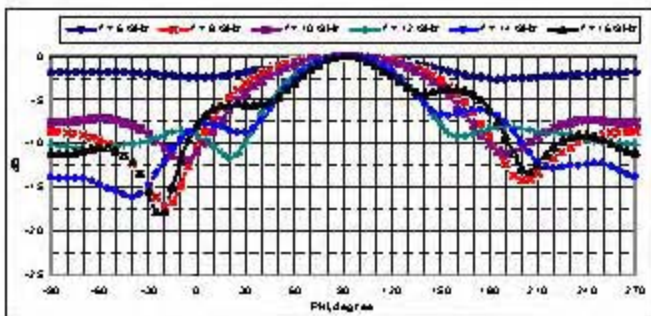


Fig. 7 Field pattern of antenna in H-plane

It can be seen from the Fig. 6 and 7 that radiation patterns in both E and H-plane are symmetrical and they both have

nearly the same beamwidth throughout the entire frequency band.

III. WIDEBAND HYBRID FOR MONOPULSE COMPARATOR

Hybrid Assembly is used to obtain monopulse sum and difference signals from individual antennas. Usually passive microwave devices are used for this purpose for example hybrid junctions and directional couplers. In this paper new type of hybrid junctions to form a monopulse hybrid assembly is proposed. Fig. 8 shows a single microstrip-slot hybrid.

The microstrip-slot hybrid is a four port device consisting of a microstrip transmission line with its 3 ports spaced and one slot line port as shown in Fig. 8. The microstrip-slot hybrid has the property that incident power at one port divides equally to the two adjacent ports inphase but no power emerges at the fourth. The power at the slot port will be divided equally to the two adjacent microstrip ports with 180° out-of-phase.

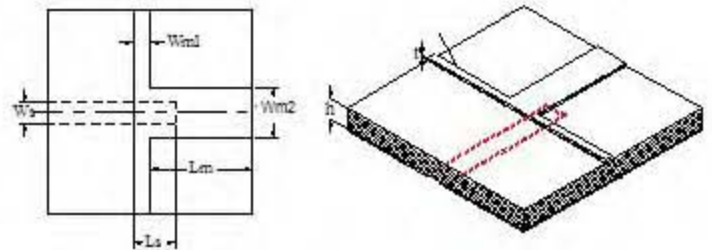


Fig. 8 Configuration of new wideband hybrid

Designed parameters of microstrip-slot hybrid with dielectric substrate ($\epsilon = 4$ (glass-bonded), $h = 1$ mm) are: $[Wm1=1.0$ mm, $Wm2=3.6$ mm, $Ls=3$ mm, $Ws=1.9$ mm, $h=1.0$ mm, $t=0.2$ mm, $\epsilon=4$].

Fig. 9 shows curves of reflection coefficients and transfer constants at four ports vs. frequency. Microwave model of this hybrid shows -140dB isolation between sum and difference channels across a 100% bandwidth.

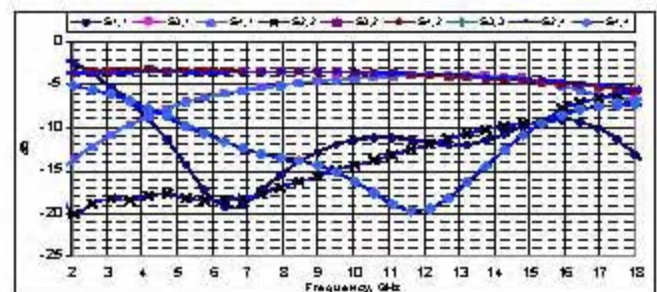


Fig. 9 Graphs of reflection coefficient and transfer constant at four ports

Phase characteristics of hybrid's ports are shown in Fig. 10. Fig. 11 depicts the voltage standing wave ratio (VSWR) of hybrid within the frequency range of 2GHz to 20GHz. It can be seen from this figure that $VSWR < 2$ within the frequency range between 5GHz and 15GHz.

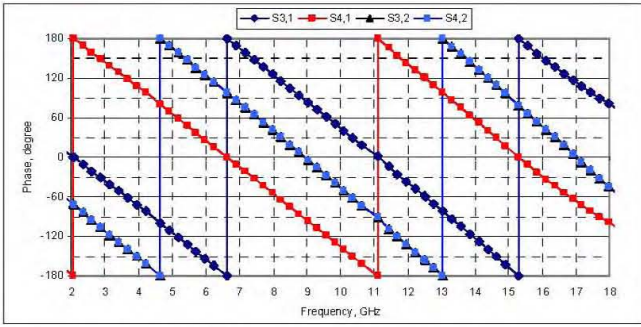


Fig. 10 Phase characteristics of hybrid

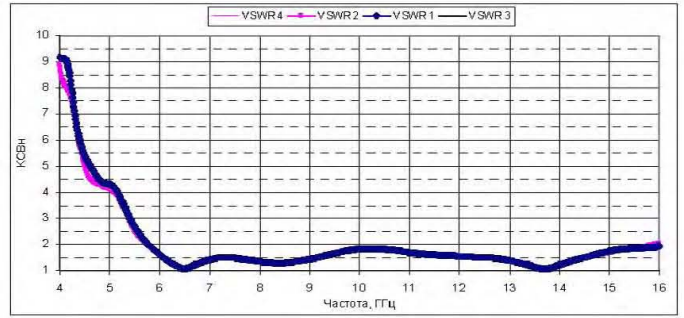


Fig. 13 VSWR vs. frequency curves

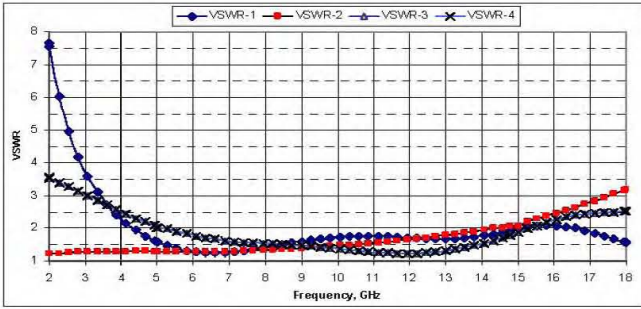


Fig. 11 VSWR vs. frequency curves

TABLE II
CHARACTERISTICS OF SUM PATTERN

f(GHz)	E-plane		H-plane		Gain (dB)
	$2\Theta_{0.7}$	SLL (dB)	$2\Phi_{0.7}$	SLL (dB)	
4	129.3	-6.5	112.7	-6.5	4.5
6	67.9	-18.4	67.8	-18.4	8.4
8	54	-19.0	51.4	-22.9	11
10	36.5	-10.2	40.5	-11.1	12.3
12	30	-8.4	32.7	-9.2	13
14	29.4	-12.3	28.4	-7.6	14
16	23.2	-7.0	24.2	-7.5	13.5

IV. WIDEBAND MONOPULSE ARRAY

Radiating part of monopulse antenna system from four double-sided tapered slot antennas is shown in Fig.12. Array distance between elements in z-axis is 20mm and that of y-axis is also 20mm.

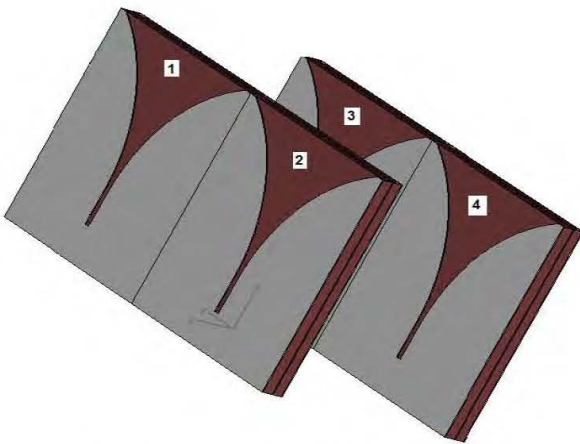


Fig.12 Radiating part of monopulse array structure

Fig. 13 shows the voltage standing wave ratio of array through the wide frequency band. $VSWR < 2$ within the frequency range 6-16 GHz.

Characteristics of the sum pattern of the wideband monopulse array are shown in Table 2. Maximum gain of array is 14 dB at 14 GHz and minimum side lobe level is -19 dB.

Fig. 14 and Fig. 15 show the sum radiation patterns in E and H-plane respectively through the frequency band from 6-16 GHz.

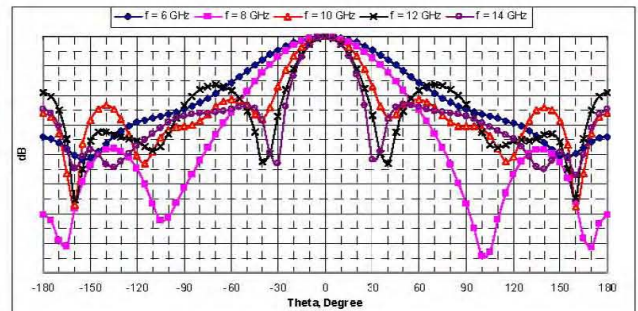


Fig. 14 Field pattern of monopulse array in E-plane (Σ channel)

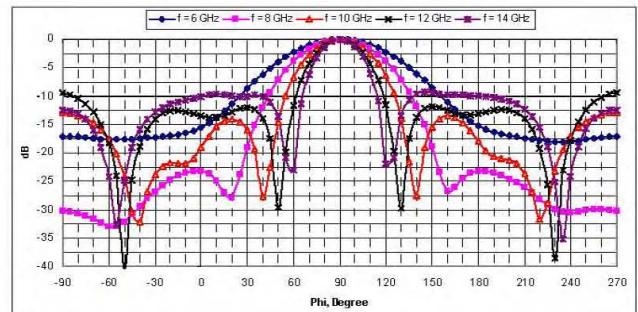


Fig. 15 Field pattern of monopulse array in H-plane (Σ channel)

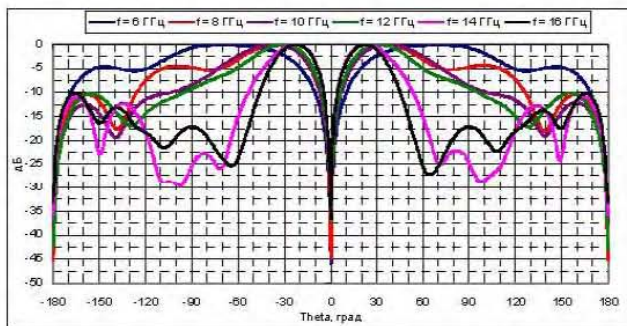


Fig. 15 Field pattern of monopulse array in E-plane (Δ channel)

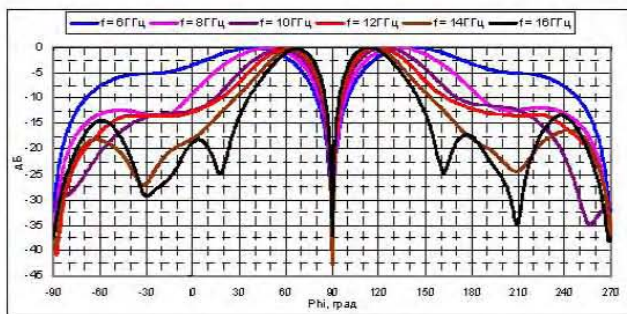


Fig. 16 Field pattern of monopulse array in H-plane (Δ channel)

Difference field patterns will be formed with 180° out-of-phase excitation in E-plane (see Fig. 15) and H-plane (see Fig. 16): $F_{\Delta E}(\theta, \phi) = [F_1(\theta, \phi) + F_3(\theta, \phi)] - [F_2(\theta, \phi) + F_4(\theta, \phi)]$ and $F_{\Delta H}(\theta, \phi) = [F_1(\theta, \phi) + F_2(\theta, \phi)] - [F_3(\theta, \phi) + F_4(\theta, \phi)]$ respectively.

Characteristics of difference patterns are shown in Table 3.

TABLE III
CHARACTERISTICS OF DIFFERENCE PATTERNS

f(GHz)	E-plane			H-plane		
	$2\Theta_{0.7}$ (deg)	Gain (dB)	Null depth (dB)	$2\Phi_{0.7}$ (deg)	Gain (dB)	Null depth (dB)
6	79	5.7	-46	63	6	-32
7	93	6.4	-39	56	7.3	-29
8	44	8	-45	49	8.3	-36
9	42	9	-43	47	8.5	-35
10	45	9.3	-37	41	9.4	-31
11	41	10	-37	37	10.6	-37
12	36	10.3	-37	34	11	-38
13	31	11	-44	31	12	-35
14	28	11	-36	30	12.3	-43
15	24	11	-37	29	12.3	-45
16	23	11	-37	27	12	-37

Sum and difference patterns of monopulse array present identically same beam width through the entire frequency band. Moreover difference patterns possess very good null depth (better than -30 dB).

Fig. 17 shows the complete monopulse hybrid assembly to produce sum and difference channel signals at the operating frequency. Four microstrip-slot hybrids can be combined to form a monopulse sum, delta azimuth and delta elevation signals.

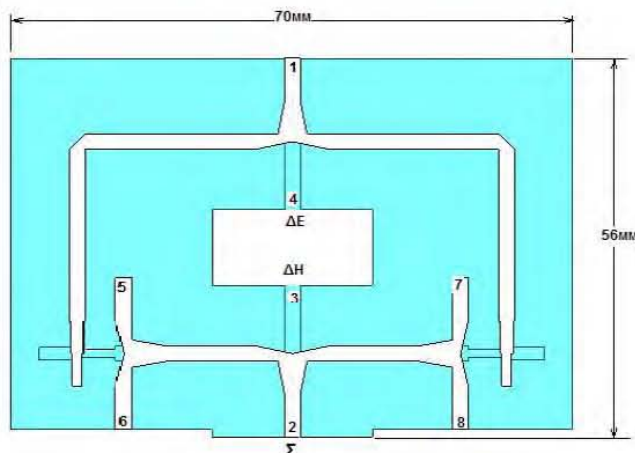


Fig. 17 Monopulse comparator for wideband array

V. CONCLUSION

In this paper a wideband monopulse array that can be used for monopulse systems in X-band is proposed. The structure is simple, light weight, low cost and easy to fabricate by photoetching, conformal installation and possess compatibility with microwave integrated circuits (MIC). The feeding comparator circuit with new type of microstrip-slot hybrid has been proposed and designed. After designing available elements of array and beam forming network, complete structure of monopulse array has been designed. Although I tried to simplify construction of the monopulse array, it will be a real challenge to realize on practice, since complete structural design of this kind involves a lot of details to be taken care of. All design procedure and choices were made after thoroughly studies of different alternatives and theory behind the problem of this paper.

REFERENCES

- [1] Сканирующие антенные системы СВЧ. Перевод с английского под редакцией Г. Т. Маркова и А. Ф. Чаплина. – М.: Издательство «Советское Радио», 1966. – 536 с.: ил.
- [2] S. M. Sherman, *Monopulse Principles and Techniques*. Dedham, MA: Artech House, 1984.
- [3] Naveed Ahsan and Jahangir Khan Kayani. Design of an X-band microstrip monopulse antenna for monopulse tracking radar. – 2nd International Bhurban Conference on Applied Sciences and Technology, Bhurban, Pakistan, 16–21 June, 2003.
- [4] Hao Wang, Da-Gang Fang and X. G. Chen. A compact single layer monopulse microstrip antenna array. - *IEEE Transactions on antennas and propagation*, 2006, vol. 54, no. 2, pp. 503-509.
- [5] Lewis, L., R., Fasset, M., Hunt, J., "A Broadband Stripline Array Element", *IEEE Symp. Antennas and Propagation*, Atlanta, USA, 1974, Pp. 335-337.
- [6] Воскресенский Д.И., Кременецкий С.Д., Гринев А.Ю., Котов Ю.В., "Автоматизированное проектирование антенн и устройств СВЧ", Москва, Радио и связь, 1988, Глава 2.